

# Investigation of the electronic properties of sodium-tungsten bronzes

N. N. Garif'yanov, V. Yu. Maramzin, G. G. Khaliullin, and I. A. Garifullin

*Kazan' Physicotechnical Institute, Kazan' Scientific Center of the Russian Academy of Sciences,  
420029 Kazan', Russian*

(Submitted 22 August 1994)

Zh. Eksp. Teor. Fiz. **107**, 556–567 (February 1995)

The magnetic susceptibility, EPR, and resistivity of sodium-tungsten bronze  $\text{Na}_x\text{WO}_3$  samples, doped with a small quantity of gadolinium, were measured. From the temperature dependence of the magnetic susceptibility contributed by the  $\text{Gd}^{3+}$  ions, it was concluded that antiferromagnetic correlations appear in the conduction band at sodium concentrations corresponding to the superconducting composition. A combined analysis of the behavior of the intensity of the EPR signal and resistivity of samples suggested that in samples with  $x=0.2$  at 2 K a phase transition occurs together with the formation of a state with spatially nonuniform electric properties. The results obtained are discussed from the standpoint of theories based on the presence of partial nesting at the Fermi surface. © 1995 American Institute of Physics.

## 1. INTRODUCTION

Sodium-tungsten bronze belongs to a group of nonstoichiometric compounds with the general formula  $\text{M}_x\text{WO}_3$ , where  $0 < x < 1$  and M is a metal. Depending on the sodium content and the preparation conditions, this compound crystallizes in the cubic, tetragonal, or orthorhombic phase.<sup>1</sup> Sodium-tungsten bronze with a tetragonal structure is the first metal oxide in which superconductivity was discovered.<sup>2</sup> The discovery of high-temperature superconductivity stimulated a reinterpretation of the experimental facts concerning the previously known metal-oxide compounds. For example, analyzing the experimental data on the physical properties of bronzes, one can see several analogies in the evolution of the electronic properties of this system and high- $T_c$  metal oxides accompanying a change in the composition. This analogy can be demonstrated for the example of  $\text{Na}_x\text{WO}_3$  and  $\text{La}_{2-x}\text{Sr}_x\text{CuO}_4$ . As  $x$  increases, a transition is observed for both systems from the dielectric state to a phase which is superconducting at low temperatures; as  $x$  increases further, the temperature of the superconducting transition passes through a maximum. Then the superconductivity vanishes and the metallic properties remain. Thus, there is a similarity in the behavior of the electric properties of these systems as a function of the composition. At the same time, their magnetic properties exhibit significant differences. For example, the parent compound  $\text{La}_2\text{CuO}_4$  is an antiferromagnet with a high Néel temperature. It is believed (see, for example, Ref. 3) that strong antiferromagnetic correlations in the conduction band also remain after doping and play an important role in the appearance of high-temperature superconductivity. In the case of sodium-tungsten bronzes, however, the parent compound  $\text{WO}_3$  is nonmagnetic. In spite of this, in recent works<sup>4–5</sup> we obtained data indicating that the antiferromagnetic correlations become stronger in the conduction band of  $\text{Na}_x\text{WO}_3$  at sodium concentrations corresponding to the superconducting composition ( $0.2 < x < 0.35$ ). It is possible that the intensification of these correlations and the appearance of superconductivity in this region is not accidental and occurs for some general

reason. The present work is an attempt to shed light on this question. We present below measurements of the magnetic susceptibility, EPR, and resistivity of samples of sodium-tungsten bronze. Gadolinium impurity is used as a magnetic probe.

The paper is organized as follows. In Sec. 2 the sample preparation and experimental procedures, employed in the investigation, are described. The experimental results on the magnetic susceptibility, EPR, and resistivity are presented in Sec. 3. Section 4 contains an analysis of the data obtained. The results are discussed in the last section.

## 2. EXPERIMENTAL PROCEDURE

*Sample preparation.* To prevent the preparation conditions from influencing the results of investigations, the samples were synthesized by two different methods. In the first method, single-crystalline samples were prepared and in the second method ceramic samples were prepared.

Single-crystalline samples were prepared by electrolysis of a melt consisting of the mixture of  $\text{Na}_2\text{WO}_4$  and  $\text{WO}_3$  in corundum crucibles by the method described in Ref. 1. The initial components were 99.999 wt.%  $\text{Na}_2\text{WO}_4$  and 99.99 wt.%  $\text{WO}_3$ . The electrodes were made of tungsten rods with a purity of 99.9 wt.%. The value of  $x$  in the single crystals obtained was fixed by the ratio of the initial components and the temperature of the charge. Dark blue needle-like single crystals with a tetragonal structure with  $x$  ranging from 0.18 to 0.3 had dimensions of  $\sim 1 \times 1 \times 5 \text{ mm}^3$ . Cubic crystals ( $0.4 < x < 0.9$ ) had a characteristic cubic faceting; their dimensions were approximately  $4 \times 4 \times 4 \text{ mm}^3$ . Gadolinium impurity was introduced by adding gadolinium tungstate  $\text{Gd}_2(\text{WO}_4)_3$  to the charge. The sodium concentration in the single crystals of the cubic phase was determined from the lattice constant by means of the relation of Brown and Banks,<sup>6</sup> which relates the value of  $x$  in  $\text{Na}_x\text{WO}_3$  and the lattice constant. For the tetragonal structure, the sodium content was obtained from the Shanks diagram,<sup>1</sup> which relates the value of  $x$  to the molar ratio of the components of the mixture of  $\text{Na}_2\text{WO}_4$  and  $\text{WO}_3$  at fixed temperature.

Ceramic samples were prepared by the Straumanis method,<sup>7</sup> in accordance with which the initial components—sodium tungstate Na<sub>2</sub>WO<sub>4</sub>, tungsten trioxide WO<sub>3</sub>, and a fine powder of tungsten metal W—were mixed and carefully ground in an agate mortar. The initial components were of the same purity as the components used for preparing single-crystalline samples. The mixture was obtained was heated in a corundum crucible in an atmosphere of pure helium up to a temperature of 1000 °C at a rate of 100 °C/h; it was held for 2 h at this temperature and then cooled at a rate of the order of 10 °C/h. It is believed<sup>7</sup> that the reaction proceeds according to the formula



The gadolinium impurity was introduced by adding to the initial mixture an appropriate quantity of gadolinium tungstate. For  $x$  ranging from 0.14 to 0.3 the sodium-tungsten bronze samples had a tetragonal structure. The product obtained was subjected to detailed x-ray analysis. The existence of only peaks belonging to sodium-tungsten bronze in the diffraction pattern shows that during preparation all components of the mixture reacted without forming a residue. Therefore, the values of  $x$  in the samples obtained by this method corresponded precisely to the computed value. As a result, we used this method of synthesizing tetragonal samples of sodium-tungsten bronze to perform detailed investigations of the composition dependence of the different parameters.

The magnetic susceptibility was measured by Faraday's method in a magnetic field of ~1 kOe. As a rule, the measurements were performed at temperatures ranging from 4.2 K up to 300 K. The temperature was measured with a AuFe–Cu thermocouple, which was placed directly adjacent to the sample. In separate cases, the investigations were performed down to temperatures of 1.8 K. The apparatus was calibrated according to a reference sample—mercury cobalt tetrathiocyanate HgCo(CNS)<sub>4</sub>, whose magnetic susceptibility is known with high accuracy.<sup>8</sup> The mass of the experimental samples was limited by the volume of the low-temperature cell. For the optimal mass of Na<sub>x</sub>WO<sub>3</sub> for our apparatus, of the order of 300 mg, the error in measuring the susceptibility did not exceed ±1% for  $\chi = 10^{-5}$  cm<sup>3</sup>/g, ±2% for  $\chi = 10^{-6}$  cm<sup>3</sup>/g, and ±10% for  $\chi = 10^{-7}$  cm<sup>3</sup>/g. The measurements were conducted in a quartz ampul, whose susceptibility was taken into account when the results obtained were analyzed. In the case when measurements were performed on single-crystalline samples, several single crystals were used to achieve the required mass.

The EPR measurements were performed on a Bruker BER-418<sup>S</sup> radiospectrometer at a frequency of 9.4 GHz in the temperature range 1.6–100 K.

The resistivity was measured by a four-contact method. The contacts were attached using gallium solder at points which were prepared by the method of ultrasonic scaling.

TABLE I. Parameters of the experimental samples Na<sub>x</sub>Gd<sub>y</sub>WO<sub>3</sub>.

Samples	$x$	$y \cdot 10^3$	$\Theta^{**}, \text{K}$	$C \cdot 10^5 \text{ cm}^3 \cdot \text{K/g}$
Ceramic				
K11	0.14	2	0	6.5
K12	0.20	2	0	6.5
K21	0.14	4	-1	13.1
K22	0.18	4	-2.5	13.1
K23	0.2	4	-6.5	13.1
K24	0.23	4	-2	13.1
K25	0.26	4	-1	13.1
K31	0.14	6	-4	19.6
K32	0.18	6	-7.5	19.6
K33	0.2	6	-8.5	19.6
K34	0.23	6	-7	19.6
K35	0.26	6	-6	19.6
K36	0.29	6	-3.5	19.6
Single-crystalline				
M11	0.18	3	-3	9.8
M12	0.20	3	-11	9.8
M13	0.3	3	-3	9.8
M21	0.20	4	-10	13.1
M31*	0.5	5	0	16.3
M32*	0.7	5	0	16.3

\*Samples M31 and M32 have a cubic structure, all others are tetragonal.

\*\*The values of  $\Theta$  are accurate to within ±0.5 K.

### 3. EXPERIMENTAL RESULTS

#### 3.1. Magnetic susceptibility

The temperature dependences of the magnetic susceptibility of four pure ceramic samples with a tetragonal structure and nineteen samples containing gadolinium impurity were measured (See Table I). Six of them were prepared by the method of electrolysis of melt and thirteen were prepared by solid-phase synthesis.

“Pure samples.” The susceptibilities of the tetragonal samples with different sodium content were virtually identical to within the measurement accuracy (see Fig. 1). The observed temperature dependence of the magnetic susceptibility of samples not containing gadolinium could be described by the expression  $\chi = C_0/T + \chi_0$ .

“Samples with gadolinium impurity.” To separate the magnetic susceptibility  $\chi_{\text{Gd}}$  determined by the gadolinium ions, the susceptibility of the corresponding “pure” samples of sodium-tungsten bronze was subtracted from the magnetic susceptibility of samples containing gadolinium. Figure 2 displays the characteristic temperature dependence, obtained in this manner, of the inverse magnetic susceptibility  $1/\chi_{\text{Gd}}$  of samples with tetragonal and cubic structures. These temperature curves can be described by the Curie–Weiss law  $\chi_{\text{Gd}}(T) = C/(T - \Theta)$  with the values of  $\Theta$  and  $C$  presented in Table I. Figure 3 displays  $\Theta$  as a function of the sodium content in ceramic samples with two different gadolinium concentrations. As one can see from the figure, for both gadolinium concentrations, the functions  $\Theta(x)$  exhibit a sharp maximum near  $x = 0.2$ . To have complete confidence in the

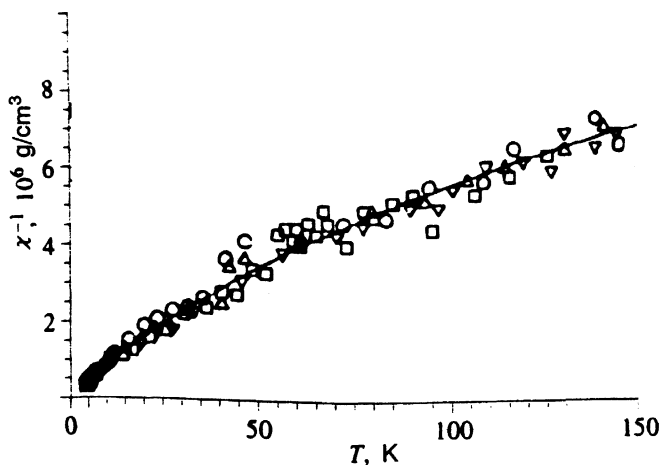


FIG. 1. Temperature dependence of the inverse magnetic susceptibility of "pure"  $\text{Na}_x\text{WO}_3$  samples:  $x=0.14$  ( $\circ$ ),  $x=0.2$  ( $\triangle$ ),  $x=0.3$  ( $\square$ ),  $x=0.29$  ( $\nabla$ ). The continuous line corresponds to the calculation using the formula  $\chi = \chi_0 + C_0/T$  with  $\chi_0 = 6 \cdot 10^{-8}$  cm<sup>3</sup>/g and  $C_0 = 1.2 \cdot 10^{-5}$  cm<sup>3</sup> K/g.

fact that nonzero values of  $\Theta$  in samples with tetragonal structure are due to gadolinium ions in a dissolved state, we measured the temperature dependence of the magnetic susceptibility of gadolinium tungstate  $\text{Gd}_2(\text{WO}_4)_3$ , through which gadolinium was introduced into the sample and whose presence in the samples cannot be completely excluded. For this compound, we obtained a value of  $\Theta$  close to zero. Generally, speaking, it also was impossible to exclude the possibility that clusters of gadolinium bronze  $\text{Gd}_x\text{WO}_3$  form the  $\text{Na}_x\text{WO}_3$  lattice. However, the investigations of gadolinium bronze  $\text{Gd}_x\text{WO}_3$  performed in Ref. 9 also gave a value of  $\Theta$  close to zero. Therefore, it can be concluded that the observed magnetic susceptibility  $\chi_{\text{Gd}}$ , described by the Curie-Weiss law with  $\Theta$  much different than zero, cannot be due to the presence of ancillary phases containing gadolinium, but rather is determined completely by the gadolinium ions in the dissolved state. The monotonic increase of  $\Theta$  and the linear increase of the Curie constant  $C$  with increasing gado-

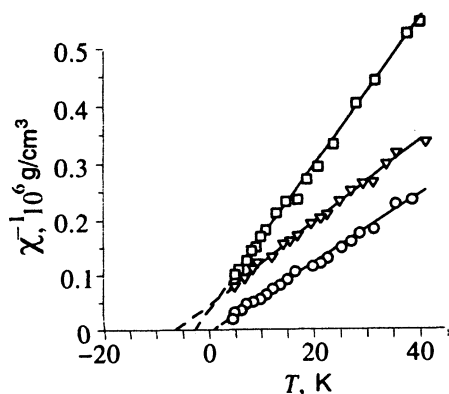


FIG. 2. Temperature dependence of the inverse magnetic susceptibility contributed by the gadolinium ions: sample M31 ( $\circ$ ), sample M13 ( $\square$ ), sample K23 ( $\nabla$ ).

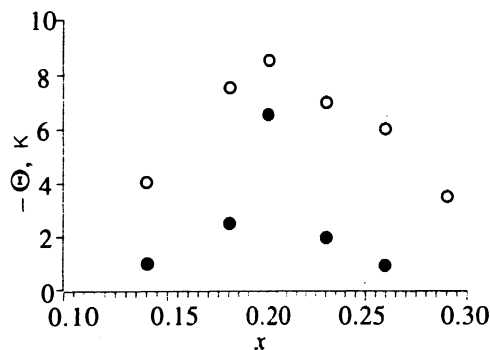


FIG. 3. Curie temperature  $\Theta$  versus the sodium content in  $\text{Na}_x\text{Gd}_y\text{WO}_3$  samples:  $\bullet$ —ceramic samples with  $y=0.004$ ;  $\circ$ —ceramic samples with  $y=0.006$ .

linium concentration indicate a more or less uniform distribution of gadolinium ions in the  $\text{Na}_x\text{WO}_3$  lattice.

### 3.2. EPR

Virtually the same EPR spectrum, displayed in Fig. 4, was observed at temperatures above 2K in all tetragonal single-crystalline samples containing gadolinium. For the ceramic samples, the spectrum was much weaker. As a result, we did not investigate EPR in them in detail. The complicated spectrum observed in samples of gadolinium-doped sodium-tungsten bronze is most likely determined by the fine structure of the  $\text{Gd}^{3+}$  ion whose environment has quite low symmetry. Besides this, the local environment, which varies from ion to ion as a result of the sodium nonstoichiometry, could complicate the spectrum. The latter fact apparently also caused the angular dependence of the spectrum to be extremely insignificant. In contrast to the strong angular dependence of the positions and intensities of different components, which is ordinarily observed for high-quality single

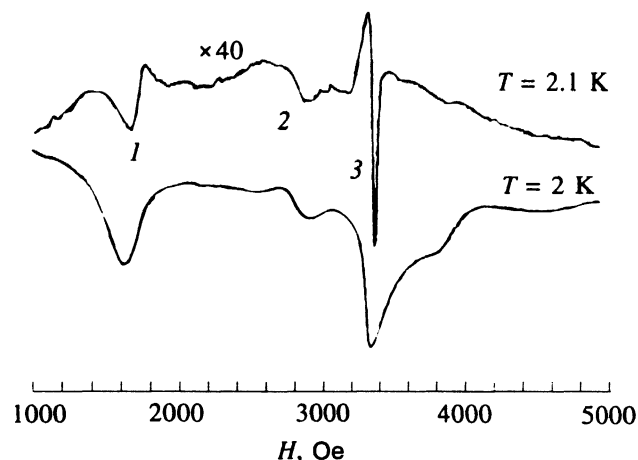


FIG. 4. EPR spectrum in sample M12 with the tetragonal axis of the crystal oriented parallel to the direction of the magnetic field.

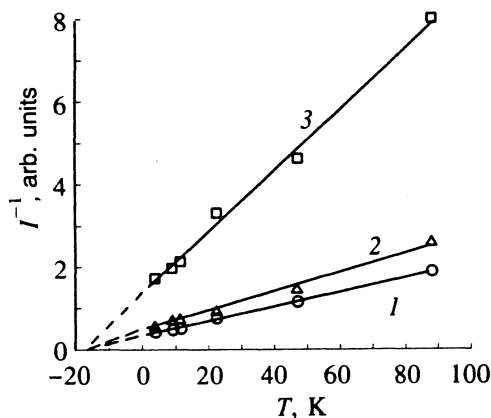


FIG. 5. Temperature dependence of the inverse integrated intensities of different lines in the EPR spectrum as marked by the numbers 1, 2, and 3 in Fig. 4.

crystals with a low density of defects, in our samples the EPR spectrum merely “breathed” slightly when the samples were rotated.

In the context of the present investigations the total intensities of the components of the EPR spectrum as a function of the temperature was most interesting. It is well known that the integrated intensity of the EPR spectrum is proportional to the static magnetic susceptibility of the spin system determining the EPR signal. In conducting samples, the intensity of the resonance signal is also proportional to the depth  $\delta$  of the skin layer. The temperature dependence of the integrated intensities of the components of the EPR spectrum for one of our experimental samples at temperatures above 4.2 K is displayed in Fig. 5. One can see from the figure that the curves are all described by the Curie–Weiss law with the same value of  $\Theta$ . Therefore, all lines in the EPR spectrum are of the same nature which apparently indicates that there were not gadolinium clusters or ancillary gadolinium-rich phases in our samples. The EPR spectrum from such inclusions would most likely consist of an isolated line with  $g \approx 2$ . This line, superposed on the line marked by the number 3 in Fig. 4, would have distorted the temperature dependence of the line, resulting in a value of  $\Theta$  which is different from that of other lines in the spectrum. Finally, the quantities  $\Theta$ , obtained from the temperature dependence of the integral intensities of the EPR lines, were found to be close to the Curie temperatures determined from the temperature dependences  $\chi_{\text{Gd}}(T)$ . This probably indicates that the magnetic susceptibility resulting from the gadolinium ions was separated correctly.

The most unexpected result of EPR was the low-temperature behavior of the EPR spectrum of samples with sodium concentration corresponding to  $x=0.2$ . As the temperature dropped below 2.1 K, a sudden rise in the intensity of the EPR signal (by approximately a factor of 40) in the range below 0.1 K occurred, superposed on a continuous change in the intensity of the EPR signal occurring in accordance with the Curie–Weiss law (see Fig. 5). Figure 4 displays the EPR spectra of the sample M12 at temperatures of 2 and 2.1 K. As one can see from the figure, besides the

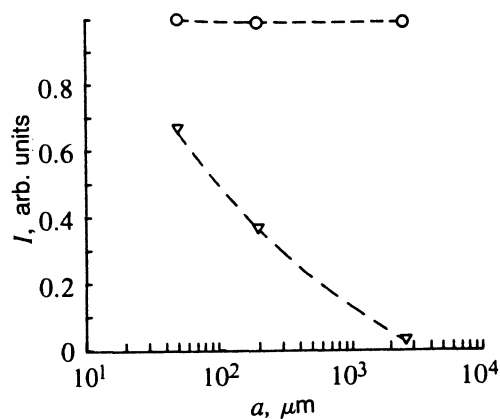


FIG. 6. EPR signal intensity in sample M12 with  $T=2$  K ( $\circ$ ) and  $T=2.1$  K ( $\nabla$ ) as a function of the size of the powder grains.

increase in the signal intensity, there is also some broadening of the components of the EPR spectrum. Similar behavior of the spectrum was also observed for the sample M21. At the same time, in tetragonal samples M11 and M13 with  $x=0.18$  and 0.3, respectively, the temperature dependence of the parameters of the EPR spectrum did not exhibit any anomalies right up to 1.6 K. Investigations showed that when samples with  $x=0.2$  are ground, the jump in the intensity near 2K decreases (see Fig. 6). One can see from Fig. 6 that the intensity of the EPR signal at  $T=2.1$  K increases as the powder particles become smaller, and at  $T=2$  K it remains practically unchanged. To determine the nature of the observed jump in the intensity of the EPR signal, we also measured the temperature dependence of the resistivity of samples in which a jump was observed in the intensity of the EPR signal near 2 K. The results of these measurements for sample M12 are presented in Fig. 7. One can see from the figure that as the temperature drops, the resistivity increases monotonically. Precise measurements of the temperature dependence of  $\rho$  at low temperatures (see inset in Fig. 7) reveal a sudden drop in the resistivity by an amount of the order of 1% at  $T=2$  K.

## 4. ANALYSIS OF THE EXPERIMENTAL RESULTS

### 4.1. Magnetic susceptibility

*Pure samples.* It can be conjectured that the Curie-like contribution to the magnetic susceptibility of “pure” samples is caused by uncontrollable magnetic impurities. A rough calculation of the possible concentration of impurities (with spin  $S=1/2$  and  $g=2$ ) gives 0.9% per formula unit. Since the total concentration of all uncontrollable impurities in the initial components is less than 0.01%, it must be concluded that the contribution under discussion cannot be attributed to uncontrollable magnetic impurities. Another reason for the appearance of a temperature-dependent contribution in the magnetic susceptibility of “pure” samples could be the presence of  $\text{W}^{5+}$  ions, which appear as a result of the localization of electrons near defects. This conjecture is based on the fact that in some of the investigated “pure” single crystals with tetragonal structure, we observed an isolated EPR line with

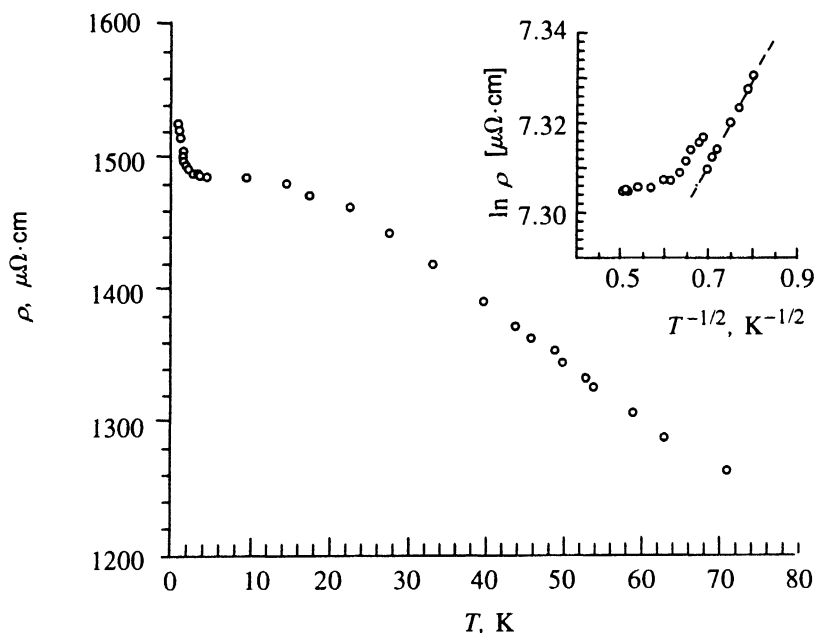


FIG. 7. Temperature dependence of the resistivity of sample M12. The dashed line in the inset corresponds to the function  $\rho \propto \exp(\sqrt{A}/T)$  with  $A = 3.6 \cdot 10^{-2}$  K.

$g=1.7$ . According to Ref. 10, where such a line was also observed, it could be due to the  $W^{5+}$  ions in the  $Na_xWO_3$  lattice.

The temperature-independent contribution  $\chi_0$  is determined by the sum of the paramagnetic contribution  $\chi_p$  of itinerant electrons and the diamagnetic core contribution  $\chi_d$ . The  $x$ -dependence of the contribution of the current carriers to  $\chi_p$  is of interest. In this connection, an attempt could be made to distinguish the different contributions to  $\chi_0$ , as done, for example, in Ref. 11. However, in our case such an analysis is of doubtful value, since  $\chi_0$  is not measured accurately enough to establish a dependence of  $\chi_p$  on the sodium content in the samples.

*Samples with gadolinium impurity.* As one can see from Table I, the value of  $\Theta$  for samples with cubic structure ( $0.5 \leq x \leq 0.7$ ) is close to zero, although the gadolinium concentration in them is higher than in tetragonal samples, where nonzero negative values of  $\Theta$  are observed. The Curie law, observed in cubic samples, shows that the exchange interactions between  $Gd^{3+}$  ions are weak. As far as the dependence of the Curie temperature  $\Theta$  on the sodium concentration in tetragonal samples is concerned, it is this non-monotonic dependence that is especially interesting (Fig. 3). The value of  $\Theta$  approaches 0 as  $x$  varies in the direction of large and small values from  $x=0.2$ . Since the gadolinium concentrations in our experimental samples are low, it is natural to conjecture that the  $Gd^{3+}$  ions interact mainly via indirect exchange through the conduction band—the Ruderman–Kittel–Kasuya–Yosida (RKKY) interaction. According to Ref. 12, the conduction band in tungsten bronzes is formed by overlapping of the  $5d$  orbitals of tungsten and the oxygen  $p\pi$  orbitals. If a simple free-electron model worked for this hybridized  $d-p$  band, then the magnitude of the RKKY interaction would depend on the sodium concentration, just as does the Pauli susceptibility. As noted above, our measurements of the susceptibility of “pure” samples are too inaccurate to record the change in the density of states

accompanying a change in the sodium concentration. According to Refs. 11, 13, and 14, where measurements of the magnetic susceptibility were conducted on samples of pure sodium-tungsten bronze with a much higher mass and in stronger magnetic fields than in our work,  $\chi_p$  is a linearly increasing function of  $x$ . In this connection, one would expect the RKKY interaction to increase monotonically with increasing sodium content. This, in turn, would result in a monotonic growth of  $\Theta$ . In reality, the function  $\Theta(x)$  has a maximum. It remains to conjecture that the free-electron-gas model is not appropriate in this case, and for  $x$  close to 0.2 strong interelectronic interactions, which increase RKKY exchange as  $x$  decreases from 0.3 to 0.2, appear in the conduction band. Since, as has already been mentioned, the homogeneous Pauli susceptibility  $\chi_p$  increases with  $x$ , it can be concluded that the observed intensification of the spin-spin interactions between gadolinium ions is due to an increase of the spin susceptibility of electrons on large wave vectors. This means that enhanced antiferromagnetic spin fluctuations in the conduction band are characteristic for compositions with sodium concentration close to 0.2.

## 4.2. EPR

The dependence of the integral intensity of the EPR signal at  $T=2.1$  K on the size of the powder grains (Fig. 6) makes it possible to estimate roughly (approximating the powder particles by spheres with the same diameter) the depth  $\delta$  of the skin layer at the working frequency of our EPR spectrometer (9400 MHz). This estimate gave  $\delta \sim 30$   $\mu\text{m}$ . Approximately the same value of  $\delta$  can be obtained from our measurements of the resistivity of this sample ( $\rho \sim 1500$   $\mu\Omega \cdot \text{cm}$ ). Therefore, at temperatures above 2 K the samples behave as ordinary conductors. We now consider the possible reasons for the jump in the intensity of the EPR

signal at 2 K. The sharp increase in the intensity of the EPR signal as a function of the temperature could be due either to a magnetic transition or a change in the character of the penetration of the microwave field into the sample. Our detailed investigations of the magnetic susceptibility did not reveal any anomalies near 2 K. This means the effect is electrical in nature. The size dependence of the intensity of the EPR spectrum (see Fig. 6) shows that at temperatures  $T \leq 2$  K the entire sample is permeated by the microwave field, i.e., at the transition near 2 K the depth  $\delta$  increases abruptly from  $\sim 30 \mu\text{m}$  up to values comparable to the sample size. For a uniform conducting system, this would mean an abrupt increase of the resistivity from  $\rho \sim 1.5 \cdot 10^3 \mu\Omega \cdot \text{cm}$  up to  $\rho \geq 10^5 \mu\Omega \cdot \text{cm}$ . At the same time, the jump present in the temperature dependence of the resistivity is small in magnitude (see inset in Fig. 7). Moreover, it occurs in a direction opposite to that expected from EPR. The narrowness of the range in which the sudden change of the resistivity and the intensity of the EPR signal occurs could indicate that a first-order phase transition occurs at  $T = 2$  K. It can be conjectured that such a transition makes the electrical properties of the sample nonuniform and the sample consists of well-conducting (metallic) and poorly conducting (dielectric) regions. In this case, the measured macroscopic conductivity no longer determines the depth of the skin layer. From the fact that at temperatures below 2 K the microwave field completely penetrates the sample, it follows that the metallic inclusions are much smaller than the characteristic depth of the skin layer determined from the conductivity. The distances between these inclusions must be large enough so as not to prevent penetration of the microwave field. For such systems one could also expect that the temperature dependence of the resistivity would be described by the law

$$\rho \propto \exp\sqrt{A/T}$$

(Ref. 15), where the parameter  $A$  is determined by the size of the metallic inclusions, the distance between them, and the permittivity of the nonmetallic regions. Naturally, we have no data on the parameter  $A$ . Nonetheless, it is evident from the inset in Fig. 7 that below 2 K the resistivity is well described by the law given above. The fact that the resistivity decreases when the sample decomposes into conducting and dielectric regions also suggests that the conducting regions consist of superconducting filaments, which, however, do not form an infinite cluster. The absence of magnetic anomalies near 2 K apparently indicates that the thickness of the superconducting filaments in the sample with  $x = 0.2$  is no greater than several hundreds of angstroms. In the opposite case, in the case of susceptibility measurements, we observed a diamagnetic contribution. It can be conjectured that the electronic phase transition occurring at 2 K is accompanied by different structural displacements. This is apparently indicated by the observed broadening of the components of the spectrum at 2 K. The absence of a jump in the intensity of the EPR signal in samples with a high sodium content apparently means that, on the one hand, the phase separation in them, if it even occurs, does so at temperatures below those we achieved. On the other hand, in such samples a sudden decrease in the intensity of the resonance signal, instead of

an increase in the signal with decreasing temperature, most likely would occur, since, as is well known,<sup>16</sup> the superconductivity in them would be of a volume character. On the basis of this picture we can understand the abrupt vanishing, observed in Ref. 16, of superconductivity in  $\text{Na}_x\text{WO}_3$  at  $x = 0.2$ . In the present work it was found that  $T_c$  increases monotonically as  $x$  decreases from 0.35 to 0.2. Then, at  $x = 0.2$ , after the maximum value of  $T_c$  was reached, the superconductivity of the sample vanished abruptly. In accordance with the picture proposed above, it can be conjectured that at  $x = 0.2$  only bulk superconductivity vanishes, and the superconducting filaments do not penetrate through the sample. To remove the apparent contradiction between the EPR data and the resistivity data we therefore assume that at 2 K the sample with  $x = 0.2$  decomposes into dielectric regions and superconducting filaments. It is precisely for this sodium content that a tendency toward a transition into a state with nonuniform electric properties is manifested. This could be associated with an increase in the scale of fluctuations of the local carrier density, the random potential of the lattice, and the localization effects for small values of  $x$ .

## 5. DISCUSSION

The main results of this work are as follows: 1) Observation of enhancement of the nonuniform spin response of the conduction band and correspondingly the indirect interaction between the magnetic impurities with sodium concentrations corresponding to  $x \sim 0.2$ ; 2) observation of a phase transition for samples with  $x = 0.2$ , presumably into a state with nonuniform electric properties. Both phenomena are absent in bronzes whose sodium content is high. It seems to us that these results can be understood on the basis of theories (see, for example, the review Ref. 17), which presuppose the existence of sections which are identical under a shift by a definite wave vector  $Q$  (nesting) on the Fermi surface. According to Mott's analysis,<sup>18</sup> the interelectronic interaction in the conduction band of  $\text{Na}_x\text{WO}_3$  is not strong enough to form Hubbard subbands, and in this sense the current carriers are not strongly correlated. To understand the enhancement of antiferromagnetic correlations, we assume that at sodium concentrations  $x \sim 0.2$  the filling of a strongly anisotropic  $d-p$  band is such that partial nesting appears on the Fermi surface. On the one hand, this intensifies the spin susceptibility near the nesting wave vector  $Q$  as a result of the effective increase of the electron-hole correlations. The enhancement of nonlocal spin response, in turn, means that the RKKY-exchange interaction between gadolinium impurities and, accordingly, the paramagnetic Curie temperature increases. On the other hand, partial nesting on the Fermi surface gives rise to electron-hole pairing and can result in partial dielectrization, accompanied also by structural transitions. Depending on the current-carrier density, the low-temperature phase can also have an elevated superconducting transition temperature as a result of a higher density of states at the Fermi level after rearrangement of the spectrum in the process of electron-hole pairing.<sup>17</sup> Our conjecture that there exists a low-temperature transition with phase

separation in our experimental samples with  $x=0.2$  fits well into this picture. We assume that in these samples spatial current-carrier density nonuniformity, associated with fluctuations in the sodium distribution, occurs. Depending on the local density of current carriers and the magnitude of the random potential, dielectric regions (with finite activation energy or localized states on the Fermi level) and metallic regions, in which superconductivity can be realized on the cluster level, apparently arise and coexist in the low-temperature phase.

The possibility of partial nesting at the Fermi surface of sodium-tungsten bronzes and the associated excitonic and structural instability were already conjectured in Ref. 17. The results of the present work apparently support this viewpoint. At the same time, the existence of nesting and enhancement of antiferromagnetic fluctuations in themselves can be important for superconductivity, as is assumed in theories of high- $T_c$  metal oxides (see, for example, Ref. 3). In this sense we cannot completely exclude the possibility that the observed enhancement of nonuniform spin susceptibility in sodium-tungsten bronze is not simply an accompanying factor precisely in the region of superconducting compositions. To clarify the possible role of spin fluctuations in the conduction band of bronzes, it is desirable to investigate the properties of the superconducting phase in detail.

This work was performed as part of project No. 91151 of the state program on high- $T_c$  superconductivity. This work is

partially supported by the International Science Fund (Grant No. NNX000).

- <sup>1</sup>H. R. Shanks, *J. Cryst. Growth* **13–14**, 433 (1972).
- <sup>2</sup>C. J. Raub, A. R. Sweedler, M. A. Jensen, S. Broadston *et al.*, *Phys. Rev. Lett.* **13**, 745 (1964).
- <sup>3</sup>J. R. Schrieffer, *Physica C* **185–189**, 17 (1992).
- <sup>4</sup>I. A. Garifullin, N. N. Garif'yanov, V. Yu. Maramzin, and G. G. Khaliulin, *Pis'ma Zh. Eksp. Teor. Fiz.* **54**, 380 (1991) [*JETP Lett.* **54**, 375 (1991)].
- <sup>5</sup>I. A. Garifullin, N. N. Garif'yanov, V. Yu. Maramzin, and G. G. Khaliulin, *Solid State Commun.* **85**, 1001 (1993).
- <sup>6</sup>B. W. Brown and E. Banks, *J. Am. Chem. Soc.* **76**, 963 (1954).
- <sup>7</sup>M. E. Straumanis, *J. Chem. Phys.* **71**, 679 (1949).
- <sup>8</sup>B. N. Figgis and R. S. Nyholm, *J. Chem. Soc.* **12**, 4190 (1958).
- <sup>9</sup>J. R. Shannon and M. J. Sienko, *Inorganic Chem.* **11**, 906 (1972).
- <sup>10</sup>H. F. Mollet and B. C. Gerstein, *J. Chem. Phys.* **60**, 1440 (1974).
- <sup>11</sup>J. D. Greiner, H. Shanks, and D. C. Wallace, *J. Chem. Phys.* **36**, 772 (1962).
- <sup>12</sup>J. C. Gulick and M. J. Sienko, *J. Solid State Chem.* **1**, 195 (1970).
- <sup>13</sup>F. C. Zumsteg, *Phys. Rev. B* **14**, 1406 (1976).
- <sup>14</sup>F. Kupka and M. J. Sienko, *J. Chem. Phys.* **18**, 1296 (1950).
- <sup>15</sup>B. Abeles, *Adv. Phys.* **24**, 407 (1975).
- <sup>16</sup>H. R. Shanks, *Solid State Phys.*, **15**, 753 (1974).
- <sup>17</sup>L. N. Bulaevskii, V. L. Ginzburg, G. F. Zharkov, D. A. Kirzhnits, Yu. V. Kopaev, E. G. Maksimov, and D. I. Khomskii, *The Problem of High-Temperature Superconductivity* [in Russian], Nauka, Moscow, 1977, Chapter 5.
- <sup>18</sup>N. F. Mott, *Phil. Mag.* **35**, 111 (1977).

Translated by M. E. Alferieff